THE JOURNAL OF BIOLOGICAL CHEMISTRY VOL. 280, NO. 40, pp. 34170–34177, October 7, 2005

Improved Photobiological H_2 Production in Engineered Green Algal Cells*

Received for publication, April 8, 2005, and in revised form, August 12, 2005 Published, JBC Papers in Press, August 12, 2005, DOI 10.1074/jbc.M503840200

Olaf Kruse[‡1], Jens Rupprecht[§], Klaus-Peter Bader[‡], Skye Thomas-Hall[¶], Peer Martin Schenk[¶], Giovanni Finazzi[‖], and Ben Hankamer[§]

From the [‡]Department of Biology VIII, Molecular Cell Physiology, University Bielefeld, 33501 Bielefeld, Germany, [‖]UPR 1261-CNRS Institut de Biologie Physico-Chimique, 75005 Paris, France, [§]Institute for Molecular Bioscience, University of Queensland, St. Lucia Campus, Queensland 4072, Australia, and [¶]Faculty of Biological and Chemical Sciences, University of Queensland, Queensland 4072, Australia

Oxygenic photosynthetic organisms use solar energy to split water (H_2O) into protons (H^+), electrons (e^-), and oxygen. A select group of photosynthetic microorganisms, including the green alga *Chlamydomonas reinhardtii*, has evolved the additional ability to redirect the derived H^+ and e^- to drive hydrogen (H_2) production via the chloroplast hydrogenases HydA1 and A2 (H_2ase). This process occurs under anaerobic conditions and provides a biological basis for solar-driven H_2 production. However, its relatively poor yield is a major limitation for the economic viability of this process. To improve H_2 production in *Chlamydomonas*, we have developed a new approach to increase H^+ and e^- supply to the hydrogenases. In a first step, mutants blocked in the state 1 transition were selected. These mutants are inhibited in cyclic e^- transfer around photosystem I, eliminating possible competition for e^- with H_2ase. Selected strains were further screened for increased H_2 production rates, leading to the isolation of *Stm6*. This strain has a modified respiratory metabolism, providing it with two additional important properties as follows: large starch reserves (*i.e.* enhanced substrate availability), and a low dissolved O_2 concentration (40% of the wild type (WT)), resulting in reduced inhibition of H_2ase activation. The H_2 production rates of *Stm6* were 5–13 times that of the control WT strain over a range of conditions (light intensity, culture time, ± uncoupler). Typically, ~540 ml of H_2 liter^{-1} culture (up to 98% pure) were produced over a 10–14-day period at a maximal rate of 4 ml h^{-1} (efficiency = ~5 times the WT). *Stm6* therefore represents an important step toward the development of future solar-powered H_2 production systems.

The development of new systems to produce zero CO_2 emission fuels for the future is one of the greatest challenges facing our society. There are two main reasons for this. First, global oil supplies are rapidly being depleted, and production levels are increasingly being reported to be close to their peak (1, 2). Second, zero CO_2 emission fuels are becoming increasingly important due to the constraints of global climate change, which is being exacerbated by anthropogenic CO_2 emissions (3–5). In this context, hydrogen is currently considered to be among the most promising clean replacement fuels for the future by a number of countries, including the United States (6), European Union,[2] and Japan.[3] Advances in fuel cell technology and the fact that the combustion of H_2 produces only H_2O increase the attractiveness of this fuel. Yet, despite the many positive aspects of a future hydrogen economy, its viability is completely dependent upon the development of efficient large scale sustainable H_2 production systems.

A select group of photosynthetic organisms have evolved the ability to harness the huge solar energy resource to drive H_2 fuel production from H_2O (9, 10) (Fig. 1*a*). Photosystem II (PSII)[4] drives the first stage of the process, by splitting H_2O into protons (H^+), electrons (e^-), and O_2. Normally, the photosynthetic light reactions and the Calvin cycle produce carbohydrates that fuel mitochondrial respiration and cell growth. However, under anaerobic conditions, mitochondrial oxidative phosphorylation is largely inhibited. Under these conditions, some organisms (*e.g. Chlamydomonas reinhardtii*) reroute the energy stored in carbohydrates to a chloroplast hydrogenase (H_2ase), likely using a NAD(P)H-PQ e^- transfer mechanism (11), to facilitate ATP production via photophosphorylation (Fig. 1*b*). Thus, H_2ase essentially acts as a H^+/e^- release valve by recombining H^+ (from the medium) and e^- (from reduced ferredoxin) to produce H_2 gas that is excreted from the cell (11). *C. reinhardtii* and potentially other green algae could therefore provide the basis for solar driven bio-hydrogen production. The combustion of the evolved H_2 yields only H_2O and thereby completes the clean energy cycle.

The hydrogenases were originally divided into three groups: the nickel-iron, the iron, and the metal-free types. However, recent data have shown that some "metal-free" hydrogenases from methanogenic Archaea actually contain a non-heme iron and CO (12), suggesting that a more complex situation might exist in nature. To date, two chloroplast H_2ases (HydA1 and HydA2) have been identified in *C. reinhardtii* (13).

Both HydA1 and HydA2 are members of the [Fe]-H_2ase class. They are monomeric in structure and have highly conserved amino acid regions containing the four cysteines (hydrogen cluster) involved in the coordination of the active center. In addition, the active center is located within a hydrophobic environment (14, 15). Apart from the hydrogen cluster, they lack any additional [Fe-S] or cysteines. Despite their relatively simple structures, these hydrogenases, which are found in green

* This work was supported by Deutsche Forschungsgemeinschaft Grant DFG-FOR387, the University of Bielefeld (to O. K), and the University of Queensland (to B. H. and J. R.). The costs of publication of this article were defrayed in part by the payment of page charges. This article must therefore be hereby marked "*advertisement*" in accordance with 18 U.S.C. Section 1734 solely to indicate this fact.

The nucleotide sequence(s) reported in this paper has been submitted to the GenBank™/EBI Data Bank with accession number(s) AF531421.

[1] To whom correspondence should be addressed. Tel.: 49-521-1065611; Fax: 49-521-1066410; E-mail: olaf.kruse@uni-bielefeld.de.

[2] European Union Commission, EU Institutions Press Releases. //europa.eu.int/rapid/start/cgi/guesten.ksh?p_action.gettxt=gt&doc=IP/02/1450 0 RAPID&lg=EN&display=.

[3] J. Koizumi (2002) *Policy Speech by Prime Minister Junichiro Koizumi to the 154th Session of the Diet*. www.kantei.go.jp/foreign/koizumispeech/2002/02/04sisei_e.html.

[4] The abbreviations used are: PSI/II, photosystem I/II; cyt, cytochrome; CCCP, carbonyl-cyanide *m*-chlorophenylhydrazone; DBMIB, 2,5-dibromo-6-isopropyl-3-methyl-1,4-benzoquinone; DCMU, dichlorophenyl dimethyl urea; HydA, hydrogenase A; H_2ase, hydrogenase; PQ, plastoquinone; Stm6, state transition mutant 6; WT, wild type; RT, reverse transcription; LHC, light-harvesting complex; Chl, chlorophyll.

algae, have a high specific activity (~1000 units/mg protein^{-1}) (16, 17). This activity is 100-fold higher than that of other H_2ases (18), highlighting the potential of *C. reinhardtii* H_2ases for the development of solar-powered hydrogen production systems.

Despite the high activities of HydA1 and HydA2, both are easily inhibited by O_2 (13). In fact, this inhibition was not overcome until 2000 when Melis and co-workers (9, 10) finally showed that the cyclical depletion and repletion of liquid *C. reinhardtii* cultures with sulfur, facilitated H_2 production from water, (+sulfur stage, PSII actively producing H^+, e^-, and O_2, H_2ases inactive; −sulfur stage, PSII inhibited, H_2ases actively recombine H^+ and e^- to produce H_2). Previous time-resolved analyses of photosynthetic protein patterns upon sulfur depletion showed a precipitous decline in the amount of ribulose-1,5-bisphosphate carboxylase-oxygenase, a more gradual decline in the level of PSII and PSI proteins, and a change in the composition of the PSII light-harvesting complex (LHC-II) (19). PSII inactivation results from the susceptibility of the D1 reaction center protein to photo-damage (20) and its inability to be repaired under sulfur deprivation. Consequently, under −sulfur conditions, the PSII-mediated water-splitting reaction and the associated O_2 evolution are inhibited. This in turn releases the oxygen inhibition of H_2ase (11).

Despite the importance of the development of the +sulfur/−sulfur system, H_2 production is limited to ~50% of its maximum capacity. This is because the H_2ase activity is inhibited during the aerobic phase. Ideally, a commercial H_2 production system would be based upon a continuous process in which PSII and H_2ases function simultaneously to drive H_2 production from water. With this aim in mind, one approach that has been pursued (with limited success to date) is the engineering of an O_2-insensitive H_2ase. However, O_2 inhibition can be considered to be a valuable attribute as it blocks continued H_2 production in the event of an accidental release of the genetically modified photosynthetic organism into an aerobic environment. Consequently, we have favored an alternative strategy; the systematic screening for mutants with an increased H^+ and e^- supply to H_2ase under anaerobic conditions. Mutants blocked in the state 1 transition were therefore selected. Normally, the state transition process regulates the light activation of PSI and PSII, by adjusting their respective light harvesting antenna sizes (21, 22). In state 1, the antenna of PSII is larger than that of PSI. In state 2 the PSII antenna size is reduced, with mobile LHC-II proteins migrating to PSI. In this way the antenna sizes of the two photosystems are adjusted, by shuttling LHC-II proteins between them (23).

In *C. reinhardtii*, state transitions have a valuable property in terms of photobiological H_2 production. This is because cyclic e^- transport is inhibited in state 1, whereas it accounts for most of the overall photosynthetic e^- flow in state 2 (24). In the WT *Chlamydomonas,* anaerobiosis induces state 2, the activation of cyclic e^- transport and therewith an additional e^- sink with which H_2ase must compete. This is likely to restrict the H_2 production capacity of the WT in sulfur-depleted anaerobic cultures (Fig. 1*b*). One solution to this problem would be to identify mutants of *C. reinhardtii* that are locked in state 1 under anaerobiosis. This approach could offer a route to eliminate the competition for PSI-derived e^-, between H_2ase and cyclic electron transport, resulting in an increased rate of e^- supply to the H_2ase.

Here we describe the development and phenotype of the state 1 blocked *C. reinhardtii* mutant *Stm6.* We also highlight the potential of this mutant as a basis upon which to develop future solar-powered H_2 production systems.

EXPERIMENTAL PROCEDURES

Generation and Identification of Stm6—Stm6 (25) is a *moc1* insertion mutant that was constructed by random gene insertion. Essentially, nuclear *C. reinhardtii* insertion mutants with modified state transition/hydrogen production properties were produced by transforming the arg^- strain (*CC1618*) with the plasmid pARG7.8 (26–30). pARG7.8 contains a 7.8-kb genomic DNA fragment of the *C. reinhardtii* arginosuccinate lyase gene. Arg^+ mutants were selected on arg^- plates (26). The arg^+ mutant library was then screened for state transition mutants (*Stm*), which were in turn screened for their ability to produce increased levels of H_2 using mass spectrometry. The phenotypic properties of *Stm6* were shown, through the detailed genetic characterization and rescue of a fully complemented stain, to be the result of knocking out the *moc1* gene (GenBank™ accession number AF531421) transcription (7). Moc1 is a novel nuclear encoded factor that is involved in the assembly of the mitochondrial respiratory chain in the light (25).

Algal Culture—WT *(CC1618)* and *Stm6* cell cultures were grown in the dark or under illumination (40–100 μmol/m^2 s^{-1} white light) on TAP (Tris (20 mM), acetate/phosphate, pH 7.0) agar plates or in TAP medium to a cell density of ~4×10^5 cells ml^{-1} (31).

Fluorescence Screening—C. reinhardtii colonies on TAP agar plates were monitored using fluorescence video imaging (Fig. 2*a*) to identify mutants blocked in state 1. Cells were pre-adapted to state 1 by illuminating with far red light (30 min, 710 nm, 10 μmol m^{-2} s^{-1}). Subsequently their ability to switch to state 2 was monitored in blue light (20 min, 480 nm, 20 μmol m^{-2} s^{-1}) as reported previously (26). Alternatively, the ability to perform state transitions was monitored by measuring changes in the fluorescence yield upon a transition from an aerobic to an anaerobic environment (23, 32, 33). Under anaerobic conditions, the plastoquinone pool is reduced by using cellular reducing power (34, 35), and activation of the kinase responsible for LHC-II phosphorylation can occur in the dark (reviewed in Ref. 32).

Spectroscopy—Cyclic e^- transport rates (Fig. 2*b*) were determined spectroscopically using a home-built spectrophotometer, described previously (24). The light-induced redox changes of cytochrome (Cyt) *f* were calculated as the difference between the absorption at 554 nm and a base line drawn between 545 and 573 nm (24). Continuous light was produced by a diode laser (SDL-LDI 3225, Wavelength Electronics) providing a 500-milliwatt emission peak at 690 nm. The light source was passed through a neutral density filters to deliver ~500 μmol m^{-2} s^{-1}. State 1 was obtained through dark incubation of the cells under aerobic conditions induced by strong agitation of the culture, whereas state 2 was induced through anaerobiosis (23). Where indicated, 20 μM dichlorophenyl dimethyl urea (DCMU) or 5 μM 2,5-dibromo-6-isopropyl-3-methyl-1,4-benzoquinone (DBMIB) was added to the solution. DCMU inhibits e^- transport from PSII to Cyt b_6f, whereas DBMIB blocks e^- transport from plastoquinone to Cyt b_6f.

Active PSI and PSII complexes were quantified spectroscopically using charge separation measurements, induced by single turnover flash excitation (Fig. 4). PSI and PSII charge separation was measured as a function of the electrochromic signal at 515–545 nm, after excitation with a saturating laser pulse (5 ns, 6 mJ at 695 nm). The PSII contribution was calculated based on the difference between the signal measured in the absence and in the presence of the PSII inhibitor DCMU. Hydroxylamine (1 mM) was added to inactivate the manganese cluster, thereby slowing down recombination between the donor and acceptor side of PSII. This increased the accuracy of the calculated PSI/PSII ratio (36). Measurements were performed either in cells that were dark-adapted for 2 h (PSII-D) or illuminated for 10 min with 200 μmol m^{-2} s^{-1} white light (PSII-L).

RNA Isolation and cDNA Synthesis—Total RNA was isolated from *C. reinhardtii* cultures using a Promega™ SV RNA isolation kit. Total RNA concentration was measured using a spectrophotometer. First strand cDNA was synthesized using 2.5 μg of total RNA in a reaction volume of 20 μl using the SuperScript III™ RT (Invitrogen) protocol. A combination of oligo(dT) (0.2 μl of 100 μM) and random hexamers (0.05 μl of 3 μg/μl) primers were used. Following synthesis, cDNA was diluted to 0.25 ml (10 ng/μl).

RT-Quantitative-PCR Conditions and Analysis—Primers were designed using the Primer Express 1.5 software (PerkinElmer Life Sciences). Actin forward primer (FP), ACGGCCAGATGATCACCATC; reverse primer (RP), AGTTGAAGGTGGTGTCGTGGAT. hydA1 (FP), AGGCTGACCGCGACTGGT; (RP),GCGCTCCTTGAAGATGTTGC. HydA2 (FP), TGGACGAGCGCAACACG; (RP) CACGTAGTGGGTGTGCAGCA.

Analysis was carried out in optical 96-well plates using an ABI PRISM 7700 sequence detector system. Each reaction contained 12.5 μl of SYBR® Green 2× Master Mix (Applied Biosystems), 20 ng of cDNA, and 280 nM of each gene-specific primer pair to a final volume of 25 μl. PCR cycling conditions consisted of an initial polymerase activation step at 95 °C for 10 min followed by 45 cycles at 95 °C for 15 s and 59 °C for 1 min, and a final melt step of 60–95 °C over 20 min. Dissociation profiles of the PCR products were analyzed with Dissociation Curves software by ABI. Real time DNA amplification was monitored and analyzed using the Sequence Detector 1.9.1 program (PerkinElmer Life Sciences). Gene expression levels relative to the housekeeping gene *actin* (D50838) were calculated for each cDNA sample using the equation: relative $\text{ratio}_{\text{gene/actin}} = (E_{\text{gene}}{}^{(-Ct\text{gene})})/(E_{\text{actin-2}}{}^{(-Ct\text{actin-2})})$. To ensure that samples are taken to the appropriate time points, the oxygen levels in the cultures were measured with a D130 data logger system using SZ10T DO electrodes (Consort, Belgium).

Hydrogen Evolution Measurements—For short term hydrogen production measured by gas mass spectrometry, 3 ml of WT and *Stm6* cell cultures (OD_{750} ~0.8) were dark-adapted for 30 min in a weak vacuum to deplete the medium and head space of O_2 and H_2 using a home-built vessel, which was directly connected to a Delta Finnigan MAT gas mass spectrometer. H_2 evolution was induced by illuminating samples either with pulsed white light (Fig. 2*C,* 3.3 Hz frequency, 12 flashes of 5 μs; 2000 μmol m^{-2} s^{-1}) or with continuous white light over a range of light intensities (Fig. 3*a,* 1 min, 15–3000 μmol m^{-2} s^{-1}). To measure H_2 production in the presence of the uncoupler CCCP, WT and *Stm6* samples were supplemented with 5 μM CCCP and subsequently illuminated with continuous white light (Fig. 3*b,* 5 min, 150 μmol m^{-2} s^{-1}).

Long Term H_2 Production Measured by Gas Chromatography—To conduct comparative studies with WT and *Stm6* cultures, both strains were grown in sulfur-replete TAP medium to a density of OD_{750} 1.0.(Chl concentration = ~13 μg/ml). To improve further the H_2 production rate of the mutant *Stm6*, cultures were grown to a higher density (OD_{750} 1.1, Chl concentration = ~26 μg/ml). The cells were then subjected to five centrifugation (3000 × *g*, 5 min, 20 °C)/wash (sulfur-free TAP medium) cycles to ensure the thorough removal of sulfur and efficient induction of the anaerobic H_2 production phase. Under continuous white light 100 μmol H_2 m^{-2} s^{-1} was produced for up to 14 days (Fig. 3*c*). The evolved gas was collected in a custom-built collecting/measurement system and injected (gas-tight lockable Hamilton syringe, SampleLock) at regular intervals into an Agilent Micro GC3000 gas chromatograph. This was fitted with a PlotU pre-column (3 m × 0.32 mm) and MolSieve 5APlot column (10 m × 0.32 mm). Argon (32.5 p.s.i.) was used as the carrier gas. Hydrogen, oxygen, and nitrogen concentrations were monitored simultaneously.

Electron Microscopy—For transmission electron microscopy, cells were grown in TAP medium to a mid logarithmic growth phase ($OD_{750\ nm}$ = 0.55) and prepared as described (37).

RESULTS

Identification of Stm6 as a State Transitions Mutant Locked in State 1—A strategy was developed to isolate random insertion mutants with an improved H_2 production capacity under low dissolved O_2 concentrations. First, *C. reinhardtii* insertion mutants were screened for a disrupted state transition process (26). This process balances the relative activities of PSI and PSII by regulating the size of their light harvesting antennae (Fig. 1, *LHC-I* and *LHC-II,* respectively). State transitions can be easily monitored by measuring the amplitude of fluorescence emission under conditions promoting either state 1 or state 2. The fluorescence emission at room temperature is inversely proportional to the yield of PSII photochemistry and proportional to the size of its light harvesting antenna (38). Thus, the large decrease of PSII antenna size, resulting from the transition from state 1 to state 2, leads to a large decrease in fluorescence (26). Indeed, such a decrease was observed in wild type cells, upon illumination with the 480 nm light (preferentially absorbed by PSII, see Fig. 2*a*) or adaptation to anaerobiosis (not shown). In contrast no such decrease was seen in *Stm6*. This indicates that *Stm6* is locked in state1. This conclusion was subsequently confirmed by 77 K fluorescence spectroscopy, which showed that (PSII) blue light illumination (480 nm) was able to increase PSI fluorescence levels at 720 nm in the wild type but not in the mutant (for details see Ref. 25).

Cyclic Electron Flow Is Down-regulated in Stm6—Previous studies in wild type *C. reinhardtii* have shown that the state transition process (state 1 to state 2) is coupled with the onset of cyclic electron flow around PSI. Thus cyclic electron flow is active in state 2 and inhibited in state 1 (24). This is clearly supported by the finding that the mutant *Stt7,* which is blocked in state 1, is unable to undergo cyclic e^- transport (24). Thus, the second screening step was designed to identify state 1 mutants (*e.g. Stm6*) that were unable to perform cyclic electron transport around PSI.

As Fig. 1*b* shows, switching off cyclic e^- transport (state 1) may potentially lift the competition for e^- between the PQ pool and H_2ase, thereby improving the rate of H_2 production. Cyclic e^- flow can be assayed by measuring the rate of Cyt *f* reduction under continuous illumination, because this complex is implicated in both (linear and cyclic) modes of electron transport. Under linear flow Cyt b_6f is reduced by PSII (via photo-generation of reduced plastoquinol (PQ)) and oxidized by PSI (via oxidized plastocyanin). In contrast, under cyclic flow, Cyt b_6f is oxidized and re-reduced by PSI alone. To determine the ratio between linear and cyclic flow, the reduction of Cyt b_6f can be measured in the presence (−DCMU) and absence (+DCMU) of PSII activity. Fig. 2*b* shows the results of this experiment for WT and *Stm6.*

In this experiment, state transitions were induced by incubating the cells either in aerobiosis (state 1) or in anaerobiosis (state 2). Both strains exhibited similar behavior under state 1 conditions. Switching the actinic light on resulted in the oxidation of Cyt *f* (Fig. 2*b, squares*), which rapidly reached a plateau level. After the light was switched off, Cyt *f* reduction was observed, and the absorption signal returned to its initial value. The oxidation yield was increased by the addition of the PSII inhibitor DCMU (Fig. 2*b, circles*) (39) or DBMIB (Fig. 2*b, triangles*), which inhibits the reduction of cytochrome *f* via PQ (reviewed in Ref. 40). As expected, this result indicates that under conditions of linear electron flow, Cyt *f* reduction is inhibited in similar measure, by blocking either PQ reduction (by PSII) or PQH_2 oxidation (by Cyt b_6f). In contrast, under state 2 conditions (anaerobiosis), the oxidation of Cyt *f* was no longer increased by the addition of DCMU (Fig. 2*b, circles*) in the wild type strain, whereas the increase was still observed in the presence

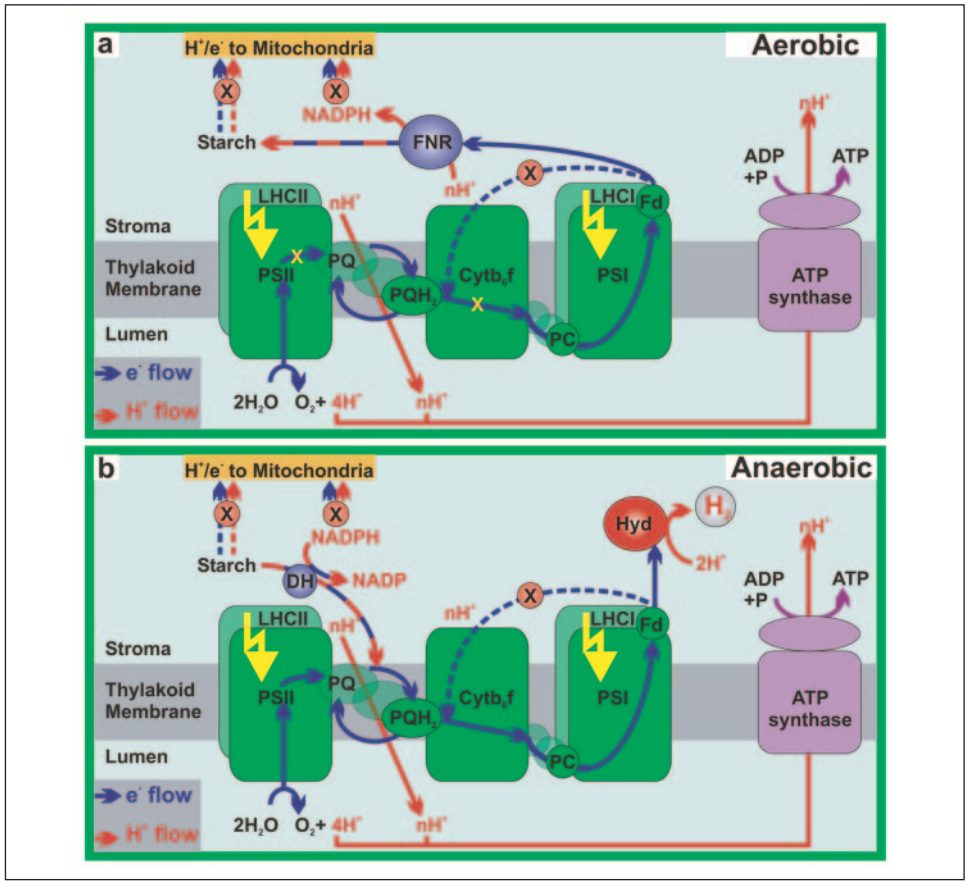

FIGURE 1. **H^+/e^- flow in the chloroplast of *C. reinhardtii* under aerobic and anaerobic conditions.** *a,* under aerobic conditions, e^- values derived from the water-splitting reaction of PSII are passed along the photosynthetic e^- transport chain (*solid blue arrows*) via plastoquinone (*PQ*), cytochrome b_6f (Cyt b_6f), photosystem I (*PSI*), and ferrodoxin (*Fd*) before being used in the production of NADPH and starch. H^+ released into the thylakoid lumen by PSII and the PQ/PQH_2 cycle (H^+ flow indicated by *solid red arrows*) generate a H^+ gradient, which drives ATP production via ATP synthase. *Dashed lines* indicate H^+ (*red*) and e^- (*blue*) transfer pathways inhibited in *Stm6*. *b,* under anaerobic conditions, H^+/e^- stored in starch and NADPH are fed to H_2ase for H_2 production. In *Stm6*, cyclic e^- transport (*dashed blue line* connecting ferredoxin (*Fd*) and Cyt b_6f) is inhibited.

of DBMIB (Fig. 2*b, triangles*). This suggests that there is a source of reducing equivalents other than PSII, which we ascribe to cyclic electron flow. This alternative path for PQ reduction was not observed in the *Stm6* mutant. Specifically, Cyt *f* oxidation levels were found to be similar in the presence of DCMU (Fig. 2*b, circles*) and DBMIB (Fig. 2*b, triangles*). These results suggest that in contrast to the WT, cyclic e^- flow is inhibited in *Stm6* because of the incapacity to perform the transition to state 2, and that PSII is the main source of reducing equivalents in the mutant under anaerobiosis.

Improved Hydrogen Production Rates in Stm6—In a final screening step, 20 strains, blocked in state1 and perturbed in cyclic electron transfer, were tested for their H_2 evolution efficiency. Hydrogen evolution capacities of WT and mutant cells cultures were measured by gas mass spectrometry in the presence and absence of sulfur. This method enabled us to monitor the composition and purity of the evolved H_2 gas (with respect to O_2 and N_2). Of these 20 strains, *Stm6* exhibited the greatest increase in H_2 production rate; a 13 times increase in short term light-driven H_2 production rate was observed in comparison with the WT (Fig. 2*c*) when monitored by gas mass spectrometry, under pulsed light illumination, which facilitates optimal PSII turn over. Moreover, short term gas mass spectrometry experiments (+sulfur, continuous illumination), also showed that *Stm6* has the potential for considerably higher H_2 production levels than the WT (Fig. 3*a*) over an illumination range of 15–3100 μmol m^{-2} s^{-1}. Under these conditions, *Stm6* consistently exhibited a ~5–7.3 times increase in hydrogen production rate over the WT.

Electron transfer in photosynthetic cells is known to promote the generation of an electrochemical proton gradient. This results in a sustained alkalinization of the stroma compartment, because of proton flux into the thylakoid lumen (41). The concomitant decrease in stromal H^+ concentration might be a limiting factor for H_2ase activity. Moreover, acidification of the thylakoid lumen might also slow down the rate of H_2 evolution, because of the inhibition of electron flow at the level of plastoquinol oxidation, as a result of the so-called "photosynthetic control" effect, as reported previously (42).

To determine whether the generation of the proton gradient inhibits the rate of H_2 evolution under aerobic conditions, the uncoupler CCCP was added to illuminated cells under (+sulfur) conditions, (*i.e.* conditions in which PSII is active and supplies H^+ into the thylakoid lumen). Fig. 3*b* shows that dissipation of the trans-thylakoid ΔpH results in a 2-fold increase in the rate of H_2 evolution in the WT, in agreement with previous reports. More importantly, a larger steady state increase (8.8 times) was observed in *Stm6*. This suggests that the rate of H_2 production in *Stm6* might be limited by the direct H^+ supply to the H_2ase.

Long Term H_2 Production Is Enhanced in Stm6—Comparative long term H_2 production experiments (14 days) in the absence of sulfur (43) were conducted using chlorophyll concentrations of 13 μg ml^{-1} (Fig. 3*c*). These conditions (triplicate samples) showed that *Stm6* produced 8.9 times more H_2 than the WT. It should be noted that the control WT strain that we used (*CC1618*) yielded less H_2 (~30–60 ml) than that reported by Melis and co-workers (~100 ml). The lower WT H_2 production levels may therefore either be strain-dependent or due to differences in experimental set up. Despite this, these results clearly demonstrate that *Stm6* has markedly improved H_2 production properties. In order to improve the H_2 production rates further, the Chl concentration was increased to ~26 μg of Chl ml^{-1}. This resulted in improved H_2 production rates in *Stm6*, resulting in the production of ~540 ml H_2 $liter^{-1}$ (up to 98% pure) by *Stm6*. The improved yield was attributed both to the higher rates (*Stm6*, 4 ml h^{-1} $liter^{-1}$ *versus* WT, 1 ml h^{-1} $liter^{-1}$, maximally) and extended period of H_2 production (*Stm6*,

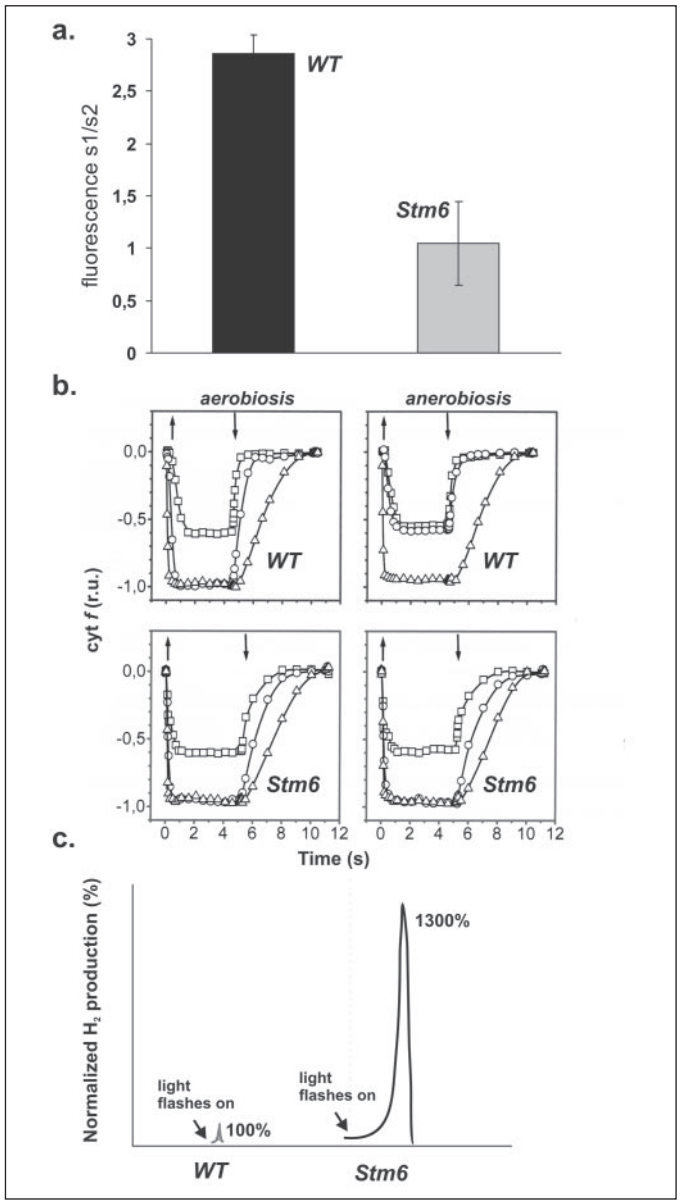

FIGURE 2. **Screening for state transition mutants of *C. reinhardtii* with improved H_2 production properties.** Identification of *Stm6* as a high hydrogen production strain. *a,* state transition activity measurements of room temperature fluorescence state 1 (*s1*)/state 2(*s2*) ratios of WT and *Stm6* cultures. Chlorophyll fluorescence intensity was detected by video imaging on state 1 (710 nm) pre-illuminated TAP agar plates light after 20 min of illumination with state 2 light (480 nm). *b,* Cyt *f* redox state changes in continuous light, as measured by absorbance changes, showing that cyclic e^- transport is fully functional in the WT but inhibited in *Stm6*. *Up arrow,* light on. *Down arrow,* light off. Absorbance decrease corresponds to oxidation of Cyt *f*. Aerobiosis induces state 1. Anaerobiosis induces state 2. A decrease in absorbance corresponds to oxidation of Cyt *f*. Traces were normalized on the amplitude of the PSI driven charge separation signal, measured at 515 nm (24). *Squares,* control; *circles,* DCMU 20 μM; *triangles,* DBMIB 5 μM. See "Experimental Procedures" for further details. *c,* hydrogen gas evolution of WT and *Stm6* cultures under pulsed light illumination (3.3 Hz frequency, 12 flashes of 5 μs; 2000 μmol m^{-2} s^{-1}) using gas mass spectrometry.

~300 h *versus* WT, ~45 h). This value is ~4–5 times higher than the highest H_2 production rates reported previously under similar culturing conditions.

More importantly, during the hydrogen evolution phase, residual oxygen evolution rates by *Stm6* remained markedly lower than those of the WT (~0.5–1% O_2 in *Stm6 versus* ~2–2.5% O_2 in WT), consistent with increased levels of H_2ase activity.

Experiments, in which DCMU (30 μM) was added to fully inhibit PSII activity, resulted in a substantial decrease (up to 85%) of H_2 production rates in both WT and *Stm6*, in agreement with earlier results (44). However whether or not this DCMU effect can be attributed to a complete deletion of any remaining e^- supply from PSII, as opposed to the non-specific inhibition of another pathway, remains to be established.

A Reduced Oxygen Concentration Is Observed in Stm6—The high H_2 production phenotype of *Stm6* was found to be based upon a complex set of mitochondrial-chloroplast interactions (25) and an altered mitochondrial metabolism. For example, *Stm6* exhibited an increased rate of oxygen consumption (data not presented) and at the same time a decreased rate of oxygen evolution due to a 30% reduction in the number of active PSII complexes under illumination with moderate light intensity (Fig. 4). The combined effect of this is that the dissolved oxygen concentration in illuminated *Stm6* cultures was only 30–40% of WT levels (~0.5–1% O_2 in *Stm6 versus* ~2–2.5% O_2 in WT).

Large Starch Deposits Are Observed in Stm6—Another important feature in terms of H_2 production is the fact that *Stm6* deposits large amounts of starch in the chloroplast (Figs. 5, *a* and *b*). Starch is reported to be used to fuel oxidative phosphorylation in the mitochondria under aerobic conditions. However, under anaerobic conditions, starch and other H^+/e^- sources can supply H^+ and e^- to H_2ase (11, 35, 45) to drive photophosphorylation in the chloroplast. The increased ability of *Stm6* to store starch appears to be linked to the inhibition of energy consumption by mitochondrial respiration under anaerobic conditions during illumination. The increased levels of stored starch are likely to be responsible for the enhanced duration of H_2 production observed in long term experiments (Fig. 3*c*).

Cellular starch levels were monitored spectroscopically ($A_{550\,nm}$) during the hydrogen production phase. A continuous decrease in the cellular starch levels was observed in both WT and *Stm6*. These results indicate that the rate of starch consumption was ~3 times higher in *Stm6* than in WT (data not presented). Furthermore, it is possible that the large starch reserves account for the increased growth rate of *Stm6* in the dark ($OD_{750\,nm}$ of 1.0–1.2 after 90 h in *Stm6 versus* 0.5–0.6 in WT after 90 h). In contrast no differences in growth rate were observed between the WT and *Stm6* when exposed to illumination levels between 5 and 200 μmol m^{-2} s^{-1}.

HydA1 and HydA2 Transcription Rates Are Not Affected in Stm6—The H_2ase transcripts of both *hydA1* and *hydA2* have been reported to be functionally expressed under anaerobic conditions (13). It was therefore important to establish whether the high H_2 phenotype of *Stm6* could be attributed at least in part to an increased level of expression of either of these two genes. To this end RT-PCR experiments were conducted (Fig. 6) These results show two things. First, that *hydA1* and *hydA2* are transcribed in both the WT and *Stm6*. Second, there is no significant difference between WT and *Stm6* in terms of the level of transcription of these two genes. These experiments clearly demonstrate that the high H_2 phenotype of *Stm6* is not the result of altered levels of HydA1 and HydA2 expression.

DISCUSSION

Our results indicate that *Stm6* has three mayor advantages for photosynthetic H_2 production. First, *Stm6* has large starch reserves that fuel photosynthetic H_2 production. Second, *Stm6* cultures exhibit lower dissolved oxygen concentrations due to reduced levels of PSII activity and increased rates of O_2 consumption. Third, inactivation of cyclic e^- transport in *Stm6* provides a permanent and fast route to supply e^- to H_2ase.

Molecular Control of Improved H_2 Production in Stm6—Engineering the optimal supply of H^+ and e^- to H_2ase is central to the development of an efficient photosynthetic H_2 production system. The results presented here clearly show that the rate of H_2 production by H_2ase can be

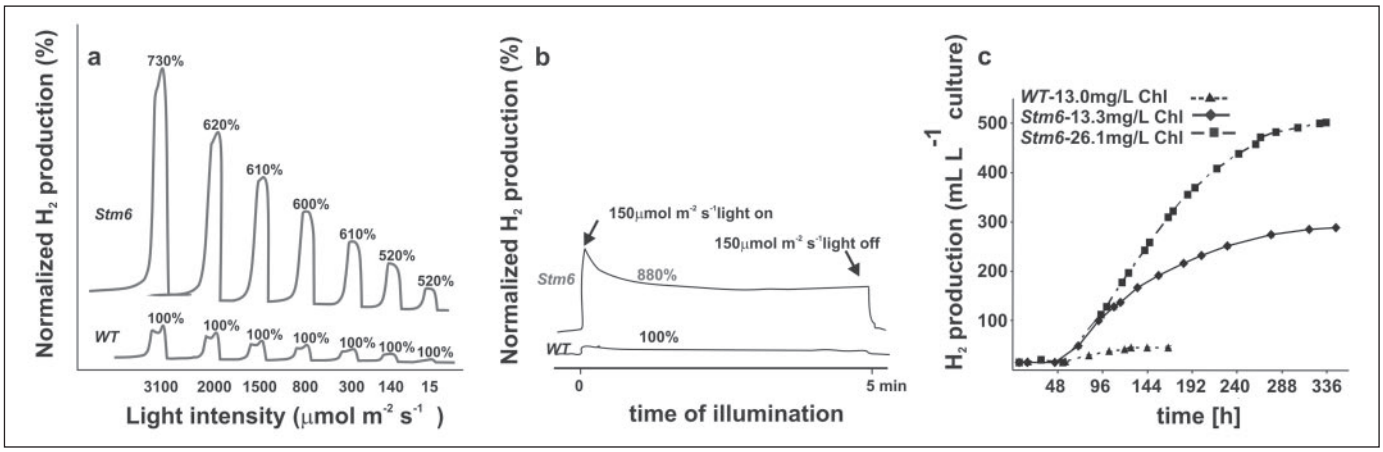

FIGURE 3. **Short and long term hydrogen production capacities in *Stm6* and WT.** *a,* short term H_2 production as a function of light intensity. In 1-min trials *Stm6* produces ~5–7 times more H_2 than the WT over a wide range of light intensities measured by gas-mass spectrometry. *b,* the effect of the uncoupler CCCP on short term H_2 production. Continuous illumination (5 min, 150 μmol m^{-2} s^{-1}) in the presence of CCCP resulted in an 8.8 times increase in steady state H_2 production in *Stm6* over the WT. CCCP addition appears to increase the flow of H^+ to H_2ase, facilitating markedly improved rates of H_2 production. *c,* long term H_2 production as a function of culture density. Under comparable culturing conditions (OD_{750} 1.0; Chl = 13.3 μg/ml for *Stm6* and 13.0 μg/ml for WT) *Stm6* produced 8.8 times the gas volume of the WT without taking into consideration the higher H_2 concentrations produced by *Stm6* during the entire duration of the H_2 evolution phase. Furthermore, under more optimal conditions (Chl concentration of the samples between 26.1 and 31.4 μg/ml), *Stm6* produces up to 540 ml/liter H_2 over a 14-day period. The composition of the gas produced by WT (average: 70.5% H_2, 2.0% O_2, 26.7% N_2) and *Stm6* (average: 92.0% H_2, 1.0% O_2, 7.0% N_2) was determined by gas chromatography. The O_2 concentration during the H_2 production phase was as follows: WT = 2.0%; *Stm6* = 1.0%. Note that the WT stops producing H_2 after ~6 days, whereas *Stm6* driven H_2 production continues until day 14.

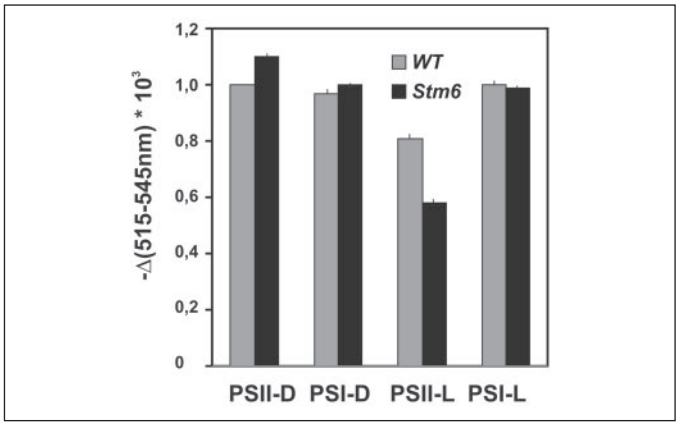

FIGURE 4. **Estimation of active PSII and PSI complexes by charge separation measurements induced by single turnover flash excitation (S.D. <0.05).** PSI and PSII activity measurements: *PSI-D* and *PSII-D*. PSI and PSII activity, dark-incubated samples (2 h). *PSI-L* and *PSII-L*. PSI and PSII activity, illuminated samples. Illumination was 10 min at 200 μmol m^{-2} s^{-1} (following a 2-h dark incubation).

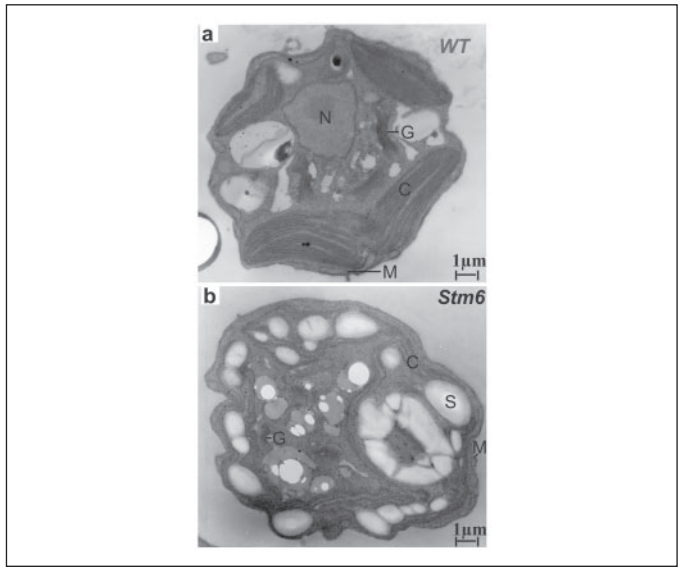

FIGURE 5. **Electron micrographs of cell sections of WT and *Stm6*.** *a,* electron micrographs of WT cell sections imaged at 20,000× magnification. *S,* starch; *M,* mitochondria; *C,* chloroplast; *G,* Golgi; *N,* nucleus. *b,* electron micrograph of *Stm6* cell section imaged at 20,000× magnification. *S,* starch; *M,* mitochondria; *C,* chloroplast; *G,* Golgi apparatus. The large starch deposits thought to act as a H^+ and e^- supply for H_2ase are of particular note.

increased by blocking the ability to perform state transitions. More precisely, blocking *C. reinhardtii* in state 1 eliminates cyclic e^- transfer and results in a marked improvement in the rate of H_2 production in the light. However, blocking cyclic e^- transport, although apparently important, is not in itself sufficient to achieve the improved rates of H_2 production observed in *Stm6*.

The semiautonomous function of the *Stm6* chloroplast, in terms of the transfer of reducing equivalents to the mitochondria, appears to be another major prerequisite for its high H_2 phenotype. (Fig. 1). The importance of this semi-autonomous function may lie in the fact that H_2ase does not have to compete for substrate with the external mitochondrial H^+ and e^- sink systems.

Under aerobic conditions *C. reinhardtii* stores the products of photosynthesis in the form of carbohydrates (Fig. 1*a*). These compounds are subsequently fed into the mitochondria to produce the ATP required to drive cellular metabolism, via F_0F_1-ATPase. In contrast, under anaerobic conditions (Fig. 1*b*), mitochondrial e^- transport is largely blocked, as complex IV is starved of O_2.

C. reinhardtii appears to have developed two mechanisms to survive anaerobic conditions. Both mechanisms ensure the ability to maintain a high ATP production capacity for a whole range of cellular processes, via the chloroplast ATP synthase. In the WT, this is particularly important, as ATP is required not only to facilitate the state 2 to state 1 transition (34) but to drive the protein synthesis, which is responsible for the recovery of photosynthetic activity during the −sulfur/+sulfur transition.

The first mechanism involves switching from linear (state 1) to cyclic (state 2) e^- transfer (Fig. 1) (32). The importance of this lies in the fact that increasing the rate of cyclic e^- transport maintains a proton gradient across the thylakoid membrane allowing ATP to be synthesized via the chloroplast ATP synthase, in the absence of mitochondrial oxidative phosphorylation.

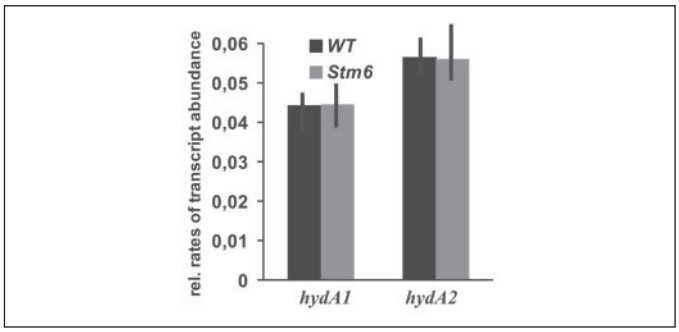

FIGURE 6. **Transcription levels of hydrogenase genes *hydA1* and *hydA2* obtained by real time RT-PCR in WT and *Stm6*.** The transcription levels are shown 10 h after the cultures reached an oxygen concentration of less than 0.1 mg/ml. Time line measurements revealed that the *hydA* expression levels reached a steady state level at this time (data not shown).

The second mechanism involves channeling the H^+ and e^- derived from starch (and from residual PSII activity) to H_2ase. These pathways were identified by the addition of the PSII inhibitor DCMU (10) and by disrupting the isoamylase gene (involved in crystalline starch accumulation), as both markedly reduced H_2 production rates (35).

In the WT optimal ATP production is dependent on active cyclic e^- transport, with more than 90% of the e^- being recycled around PSI (22). However, for the purpose of H_2 production, this is not ideal as cyclic e^- transport competes with H_2ase for e^-, limiting the rate of hydrogen production of the system. In contrast, *Stm6* is blocked in state 1 in the light and is unable to perform cyclic e^- transport, increasing substrate supply to H_2ase (Fig. 1*b*). Based on reports that at least 90% of the e^- are normally recycled around PSI, a 9 times increase over WT H_2 production rate would theoretically be expected if cyclic e^- flow were switched off. Our results show that under uncoupled conditions (Fig. 3*b*, + CCCP), in which both e^- and H^+ supply are near optimal in *Stm6*, an 8.8 times increase in the steady state H_2 production rate was indeed achieved. These results indicate that there is considerable potential to increase the rate of long term H_2 production beyond the level shown in Fig. 3*c* (~540 ml of H_2 per liter of cell culture).

Role of the Mitochondria-Chloroplast Metabolic Interactions on H_2 Production—Although the reduction of cyclic e^- transport appears to be an important factor contributing to the high H_2 phenotype of *Stm6*, it is not in itself sufficient to explain the phenotype fully as similar rates of H_2 production were not observed (data not shown) in other mutants locked in state 1, including the *Stt7* strain (33). Clearly other features of *Stm6* also contribute to its high H_2-producing phenotype. One major feature is the modified mitochondrial metabolism. Because of the disruption of the nuclear encoded *moc1* gene, *Stm6* shows reduced levels of the rotenone-insensitive NADPH dehydrogenase and increased levels of alternative oxidase (25).

The reduced ability to transport a net flux of H^+ and e^- into the mitochondrion and to use them to drive oxidative phosphorylation essentially switches off the capacity of the mitochondrion to act as a sink for the products of photosynthesis (25) (Fig. 1). This may explain the high level of starch accumulation observed in the *Stm6* chloroplast (Fig. 5, *a* and *b*) and the ability of this mutant to support the efficient and long term supply of H^+ and e^- to H_2ase under anaerobic conditions. Similar effects of a reduced cytoplasm on starch accumulation and hydrogenase supply have been observed recently in cyanobacteria (8).

The importance of the large starch supply of *Stm6*, as an e^- and H^+ supply for H_2ase, is also emphasized by a recent study that reported that disrupting an isoamylase gene caused a rapid decline in the rates of *hydA1* transcription and hydrogen evolution (35). This study is supported by our own results that showed that starch consumption rates were higher in *Stm6* than in the WT during the H_2 production phase.

A further point of note is the decreased cellular oxygen concentration of *Stm6* in the light, which facilitates the rapid induction of H_2ase activity. Consequently, with further fine-tuning of the culturing conditions, *Stm6* may be able to drive a continuous H_2 production process, with an improved e^- supply to H_2ase.

Conclusion—*Stm6* has a number of valuable attributes for the development of future solar-powered H_2 production systems capable of using H_2O as a substrate under a state of "anaerobic photosynthesis." First, the chloroplast of *Stm6* functions semi-autonomously, feeding the H^+ and e^- derived from H_2O (either directly or from starch) to H_2ase for H_2 production, rather than into the mitochondrial e^- transport chain. Second, as cyclic e^- transport is switched off in *Stm6,* this mutant provides a permanent and fast route for the supply of e^- to H_2ase. Third, *Stm6* maintains low cellular O_2 concentrations, resulting in a marked increase in H_2ase activity. For these reasons, *Stm6* is able to produce H_2 at rates 5–13 times higher than the WT in short term experiments (Fig. 2*c* and Fig. 3, *a* and *b*). Furthermore, the long term experiments (Fig. 3*c*) show that *Stm6* exhibits a ~5.4 times increase in total H_2 production yield over the WT. Recent calculations based on the long term experiments (Fig. 3*c*) suggest that at 20 μmol m^{-2} s^{-1} *Stm6* has a 1.5% photon conversion efficiency to H_2. This increase is a major step forward in the development of economically viable H_2 production systems capable of producing H_2 at rates ~50 times the WT (~5% photon conversion efficiency). The pulsed light H_2 measurements in the presence of sulfur shown in Fig. 2*c* also highlight the potential of *Stm6* to support H_2 production rates of at least 13 times that of the WT. *Stm6* is therefore a good platform for further genetic manipulation for improvement of photobiological H_2 production under both aerobic and anaerobic conditions.

Acknowledgment—We thank UniSense (Denmark) for experimental support.

REFERENCES

1. Rifkin, J. (2002) *The Hydrogen Economy*, pp. 64–91, Penguin Putnam Inc., New York
2. Deffeyes, K. S. (2001) *Hubbert's Peak: The Impending World Oil Shortage*, pp. 5–200, Princeton University Press, Princeton, NJ
3. Petit, J. R., Jouzel, J., Raynaud, D., Barkov, N. I., Barnola, J. M., Basile, I., Bender, M., Chappellaz, J., Davis, M., Delaygue, G., Delmotte, M., Kotlyakov, V. M., Legrand, M., Lipenkov, V. Y., Lorius, C., Pepin, L., Ritz, C., Saltzman, E., and Stievenard, M. (1999) *Nature* **399,** 429–436
4. Thomas, C. D., Cameron, A., Green, R. E., Bakkenes, M., Beaumont, L. J., Collingham, Y. C., Erasmus, B. F., De Siqueira, M. F., Grainger, A., Hannah, L., Hughes, L., Huntley, B., Van Jaarsveld, A. S., Midgley, G. F., Miles, L., Ortega-Huerta, M. A., Peterson, A. T., Phillips, O. L., and Williams, S. E. (2004) *Nature* **427,** 145–148
5. O'Neill, B. C., and Oppenheimer, M. (2002) *Science* **296,** 1971–1972
6. Abraham, S. (2002) *National Hydrogen Energy Roadmap,* United States Department of Energy, Washington, D. C.
7. Hankamer, B., and Kruse, O. (January 13, 2005) U. S. Patent WO2005003024
8. Cournac, L., Guedeney, G., Peltier, G., and Vignais, P. (2004) *J. Bacteriol.* **186,** 1737–1746
9. Melis, A., Zhang, L., Forestier, M., Ghirardi, M. L., and Seibert, M. (2000) *Plant Physiol.* **122,** 127–136
10. Ghirardi, M. L., Zhang, L., Lee, J. W., Flynn, T., Seibert, M., Greenbaum, E., and Melis, A. (2000) *Trends Biotechnol.* **18,** 506–511
11. Melis, A., and Happe, T. (2001) *Plant Physiol.* **127,** 740–748
12. Lyon, E. J., Shima, S., Buurman, G., Chowdhuri, S., Batschauer, A., Steinbach, K., and Thauer, R. K. (2004) *Eur. J. Biochem.* **271,** 195–204
13. Forestier, M., King, P., Zhang, L., Posewitz, M., Schwarzer, S., Happe, T., Ghirardi, M., and Seibert, M. (2003) *Eur. J. Biochem.* **270,** 2750–2758
14. Peters, J. W., Lanzilotta, W. N., Lemon, B. J., and Seefeldt, L. C. (1998) *Science* **282,** 1853–1858
15. Peters, J. W. (1999) *Curr. Opin. Struct. Biol.* **9,** 670–676
16. Happe, T., and Naber, J. D. (1993) *Eur. J. Biochem.* **214,** 475–481
17. Florin, L., Tsokoglou, A., and Happe, T. (2001) *J. Biol. Chem.* **276,** 6125–6132

18. Adams, M. W. W. (1990) *Biochim. Biophys. Acta* **1020,** 115–145
19. Zhang, L. P., Happe, T., and Melis, A. (2002) *Planta* **214,** 552–561
20. Barber, J., and Andersson, B. (1992) *Trends Biochem. Sci.* **17,** 61–66
21. Murata, N. (1969) *Biochim. Biophys. Acta* **172,** 242–251
22. Bonaventura, C., and Myers, J. (1969) *Biochim. Biophys. Acta* **189,** 366–386
23. Allen, J. F., Bennett, J., Steinback, K. E., and Arntzen, C. J. (1981) *Nature* **291,** 25–29
24. Finazzi, G., Rappaport, F., Furia, A., Fleischmann, M., Rochaix, J. D., Zito, F., and Forti, G. (2002) *EMBO Rep.* **3,** 280–285
25. Schönfeld, C., Wobbe, L., Borgstädt, R., Kienast, A., Nixon, P. J., and Kruse, O. (2004) *J. Biol. Chem.* **279,** 50366–50374
26. Kruse, O., Nixon, P. J., Schmid, G. H., and Mullineaux, C. W. (1999) *Photosynth. Res.* **61,** 43–51
27. Debuchy, R., Purton, S., and Rochaix, J. D. (1989) *EMBO J.* **8,** 2803–2809
28. Kindle, K. L., Schnell, R. A., Fernandez, E., and Lefebvre, P. A. (1989) *J. Cell Biol.* **109,** 2589–2601
29. Gumpel, N. J., and Purton, S. (1994) *Trends Cell Biol.* **4,** 299–301
30. Purton, S., and Rochaix, J. D. (1995) *Eur. J. Phycol.* **30,** 141–148
31. Harris, E. (1989) *The Chlamydomonas Sourcebook: A Comprehensive Guide to Biology and Laboratory Use,* Academic Press, San Diego
32. Wollman, F. A. (2001) *EMBO J.* **20,** 3623–3630
33. Depege, N., Bellafiore, S., and Rochaix, J.-D. (2003) *Science* **299,** 1572–1575
34. Bulte, L., Gans, P., Rebeille, F., and Wollman, F. (1990) *Biochim. Biophys. Acta* **1020,** 72–80
35. Posewitz, M. C., Smolinski, S. L., Kanakagiri, S., Melis, A., Seibert, M., and Ghirardi, M. L. (2004) *Plant Cell* **16,** 2151–2163
36. Finazzi, G., Chasen, C., Wollman, F. A., and de Vitry, C. (2003) *EMBO J.* **22,** 807–815
37. Engels, A., Kahmann, U., Ruppel, H. G., and Pistorius, E. K. (1997) *Biochim. Biophys. Acta* **1340,** 33–44
38. Butler, W. L. (1978) *Annu. Rev. Plant Physiol.* **29,** 345–378
39. Bennoun, P. (1970) *Biochim. Biophys. Acta* **216,** 357–363
40. Frank, K., and Trebst, A. (1995) *Photochem. Photobiol.* **61,** 2–9
41. Heldt, H. W., Werdan, K., Milovanc, M., and Geller, G. (1973) *Biochim. Biophys. Acta* **314,** 224–241
42. Bendall, D. S. (1982) *Biochim. Biophys. Acta* **683,** 119–151
43. Melis, A., and Zhang, L. (1999) *Proceedings of the 1999 United States DOE Hydrogen Program Review NREL/CP-570–26938*, pp. 1–19, United States Department of Energy, Washington, D. C.
44. Antal, T., Krendeleva, T., Laurinavichene, T., Makarova, V., Ghirardi, M., Rubin, A., Tsygankov, A., and Seibert, M. (2003) *Biochim. Biophys. Acta* **1607,** 153–160
45. Kosourov, S., Seibert, M., and Ghirardi, M. L. (2003) *Plant Cell Physiol.* **44,** 146–155